RSC Advances

PAPER

View Article Online
View Journal | View Issue

Cite this: *RSC Adv.*, 2021, **11**, 4147

Novel triazole derivatives as ecological corrosion inhibitors for mild steel in 1.0 M HCl: experimental & theoretical approach

A. Nahlé, *[a] R. Salim,[b] F. El Hajjaji,[b] M. R. Aouad,[c] M. Messali,[c] E. Ech-chihbi,[b] B. Hammouti[d] and M. Taleb[b]

The present paper illustrates the investigation of two novel ecological triazole derivative corrosion inhibitors, namely ethyl 2-(4-phenyl-1*H*-1,2,3-triazol-1-yl) acetate [Tria-CO_2Et], and 2-(4-phenyl-1*H*-1,2,3-triazol-1-yl) acetohydrazide [Tria-$CONHNH_2$]. The studied inhibitors were investigated against the corrosion of mild steel in 1.0 M HCl solution using different electrochemical techniques. Potentiodynamic polarization experiments indicated that the [Tria-CO_2Et], and the [Tria-$CONHNH_2$] acted as mixed type inhibitors. Electrochemical impedance spectroscopy measurements revealed that both inhibitors presented a high inhibition performance, achieving an inhibition efficiency of 95.3% for [Tria-CO_2Et] and 95.0% for [Tria-$CONHNH_2$] at a concentration of 1.0×10^{-3} M. Based on the Langmuir isotherm model and the activation parameters, these triazole derivatives were adsorbed onto a steel surface by physical and chemical bonds. Density functional theory based on B3LYp6-311G(d,p) was also carried out to correlate the inhibition efficiencies obtained experimentally with the theoretical descriptors of the studied molecular structures.

Received 13th November 2020
Accepted 28th December 2020

DOI: 10.1039/d0ra09679b

rsc.li/rsc-advances

1. Introduction

Generally, triazole is a five-membered ring containing three nitrogen atoms, and acts as a building block for many compounds that have various applications, especially in medicine.[1] These triazole derivative compounds have attracted wide interest from many researchers because of their exceptional properties. They have diverse agricultural, industrial, and biological properties, as well as anti-microbial, anticonvulsant, anticancer, anti-inflammatory, diuretic, antibacterial, hypoglycemic, antitubercular, and antifungal activities.[2]

Various industrial fields use construction materials such as mild steel, since it is of low cost, high availability, and good physicochemical characteristics.[3,4] However, mild steel can be easily weakened and causes wide human and economic costs when it is in contact with an aggressive acidic solution. Therefore, the best way to protect the steel surface is by applying inhibitors that act as a wall between the steel surface and the aggressive medium.[5,6] Moreover, this film barrier can be explained by the adsorption of these molecules on the metal surface using several heteroatom centers such as N, S, and O heteroatoms, and π-electrons. Furthermore, this adsorption can be achieved through physical adsorption, chemisorption, or both (physical and chemical).[7,8]

Recently, many researchers have focused on the application of eco-friendly corrosion inhibitors. These compounds can be considered as ecological inhibitors since they have low toxicity and characteristics of strong chemical activity.[9,10] These triazole derivatives are amphoteric in nature, forming salts with acids and bases, and have special affinity to metal surfaces with moving water molecules on the surface. Moreover, they have abundant p-electrons and unshared electron pairs on the nitrogen atom that can combine with d-orbitals of the metal to afford a protecting film.[11,12] Therefore, several previous works have focused on the application of 1,2,4-triazole derivatives as corrosion inhibitors.[13,14] For instance, El Belghiti *et al.* showed that two 3,5-bis (disubstituted)-4-amino-1,2,4-triazole derivatives (T1 and T2) have a corrosion inhibition efficiency of 86% for mild steel when used at a concentration of 1.0×10^{-3} M in 2 M H_3PO_4.[15] More recently, newly synthesized heterocycles, namely (1-*p*-tolyl-1*H*-1,2,3-triazol-4-yl) methanol (TTM)[16] and 5-hexylsulfanyl-1,2,4-triazole (HST),[17] have been investigated in inhibiting steel corrosion in 1.0 M HCl. These compounds displayed excellent inhibition performance. The inhibition efficiencies reached 97% for HST and 81% for TTM based on electrochemical data at 1.0×10^{-3} M. In addition, the effect of heteroatoms on the corrosion inhibition of structurally similar

[a]*Department of Chemistry, College of Sciences, University of Sharjah, P.O.Box: 27272, Sharjah, United Arab Emirates. E-mail: anahle@sharjah.ac.ae; Fax: +971-6-5053820; Tel: +971-6-5166 771*

[b]*Laboratory of Engineering, Electrochemistry, Modeling and Environment (LIEME), Faculty of Sciences, University Sidi Mohamed Ben Abdellah, Fez, Morocco*

[c]*Department of Chemistry, College of Science, Taibah University, Al-Madinah Al-Munawarah 30002, Saudi Arabia*

[d]*Laboratory of Applied Chemistry and Environment (LCAE), Faculty of Sciences, University Mohammed Premier Oujda, Morocco*

Table 1 Percentage inhibition efficiency for some selected triazole derivatives used as corrosion inhibitors against the corrosion of mild steel in an acidic medium

Triazole derivative	Inhibition efficiency (%)	Medium	Ref.
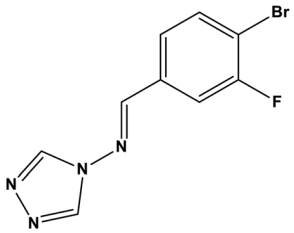 (3-Bromo-4-fluoro-benzylidene)-[1,2,4] triazol-4-yl-amine (BFBT)	85.05% at 3.2 mM	0.5 M HCl	14
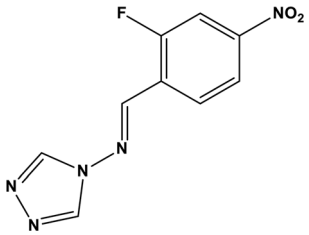 (2-Fluoro-4-nitro-benzylidene)-[1,2,4] triazol-4-yl-amine (FNBT)	72.83% at 3.2 mM	0.5 M HCl	14
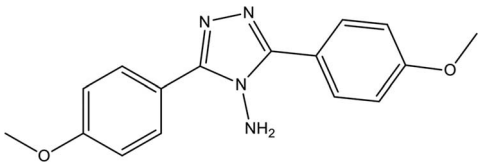 3,5-Bis(4-methoxyphenyl)-4-amino-1,2,4-triazole (T1)	86.81% at 1.0×10^{-3} M	2 M H_3PO_4	15
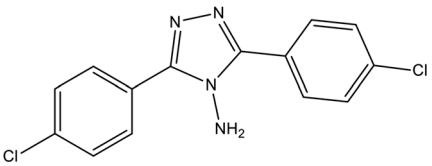 3,5-Bis(4-chlorophenyl)-4-amino-1,2,4-triazole (T2)	86.20% at 1.0×10^{-3} M	2 M H_3PO_4	15
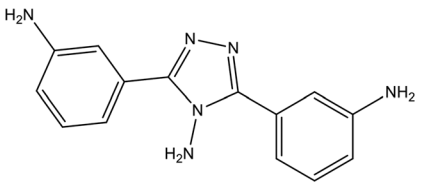 3,5-Bis(3-aminophenyl)-4-amino-1,2,4-triazole (3-APAT)	89.9% at 1.0×10^{-4} M	1.0 M HCl	16
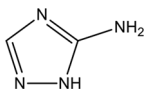 5-Amino-1,2,4-triazole (5-ATA),	24% at 1.0×10^{-2} M	1.0 M HCl	17
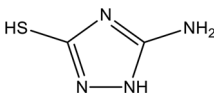 5-Amino-3-mercapto-1,2,4-triazole (5-AMT)	92% at 1.0×10^{-2} M	1.0 M HCl	17
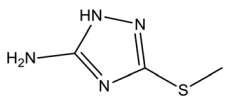 5-Amino-3-methylthio-1,2,4-triazole (5-AMeTT)	82% at 1.0×10^{-2} M	1.0 M HCl	17
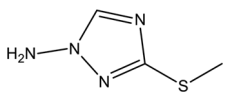 1-Amino-3-methylthio-1,2,4-triazole (1-AMeTT)	82% at 1.0×10^{-2} M	1.0 M HCl	17

Table 2 Abbreviations, structures, and IUPAC names for the studied triazole derivatives

Abbreviations	Structures	IUPAC name
[Tria-CO_2Et]	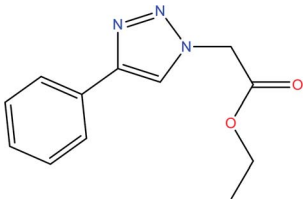	Ethyl 2-(4-phenyl-1*H*-1,2,3-triazol-1-yl)acetate
[Tria-$CONHNH_2$]	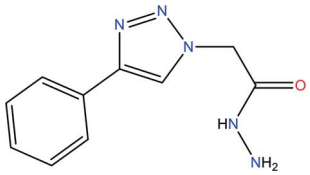	2-(4-Phenyl-1*H*-1,2,3-triazol-1-yl)acetohydrazide

azomethine-based organic molecules (FMT and TMT) showed that both molecules had good efficiency (>90%) at 5 mmol L^{-1} concentration in 1.0 M HCl medium.[18]

Many authors have reported that the quantum chemical calculations can offer broad information about structural properties and relate inhibitors' adsorption ability with their structural aspects.[19] Y. El Aoufir *et al.*[20] have established a correlation between two 1,2,4-triazole derivatives (TR8 and TR10) and their electronic properties. This investigation confirmed the strong adsorption of these inhibitors on the mild steel surface through active centers distributed over the triazole moiety and the carbon chain of the studied compounds. In addition, some other authors have used quantum chemistry calculations (density functional theory, DFT) to understand inhibitor interactions with the metal surface.[21–24] As an example, Table 1 reports the percentage inhibition efficiency for some selected triazole derivatives used as corrosion inhibitors against the corrosion of mild steel in an acidic medium.

In this work, we have investigated the effect of two novel synthesized compounds derived from triazole, namely ethyl 2-(4-phenyl-1*H*-1,2,3-triazol-1-yl) acetate [Tria-CO_2Et], and 2-(4-phenyl-1*H*-1,2,3-triazol-1-yl) acetohydrazide [Tria-$CONHNH_2$], as corrosion inhibitors. This investigation was performed on mild steel substrates using various electrochemical techniques, such as electrochemical impedance spectroscopy (EIS) and potentiodynamic polarization (PDP). DFT based calculations in the gaseous as well as in the aqueous phase were executed to correlate the quantum chemical descriptors of the triazole-derived compounds used and their experimental inhibition efficiency.

2. Experimental

2.1. Inhibitor synthesis

The click coupling of phenylacetylene (**1**) with ethylazidoacetate (**2**), in the presence of sodium ascorbate and copper sulfate as a catalyst in a mixture of *t*-BuOH : H_2O (1 : 1), gave the targeted ethyl 2-(4-phenyl-1*H*-1,2,3-triazol-1-yl) acetate (**1**) with 96% yield after stirring at room temperature for 4 h.

The structure of the 1,2,3-triazole (**3**) was elucidated based on its spectral data (IR, and ^1H and ^{13}C-NMR). Its ^1H-NMR spectrum revealed the absence of the characteristic alkyne proton (≡**CH**) and the presence of a distinct singlet at δ_H = 8.50 ppm assigned to the triazolyl C_5–H proton, confirming the success of the 1,3-dipolar cycloaddition reaction. The spectrum also revealed the presence of a triplet at 1.24 ppm and a quartet at 4.18–4.22 ppm attributed to the ethyl ester protons (C**H**$_3$) and (OC**H**$_2$), respectively. In the ^{13}C-NMR spectrum, the carbon signals belonging to **C**H_3, N**C**H_2 and O**C**H_2 resonated at δ_C 14.78, 51.31, and 63.40 ppm, respectively. The sp^2-carbons were recorded at their appropriate chemical shifts. Thermal hydrazinolysis of the resulting 1,2,3-triazole based-ester (**3**), with hydrazine hydrate for 4 h, afforded the corresponding acid hydrazide (**4**) in excellent yield (90%) (Scheme 1). The success of the hydrazinolysis reaction has been clearly evidenced based on the spectral data of compound (**4**), which revealed the disappearance of the ethyl ester protons and carbons of its starting material (**3**). The ^1H-NMR spectrum also confirmed the presence of the diagnostic hydrazide N**H**$_2$ and N**H** protons as two singlets at δ_H 4.62, and 9.58 ppm, respectively. All carbon signals related to the proposed structure of compound (**4**)

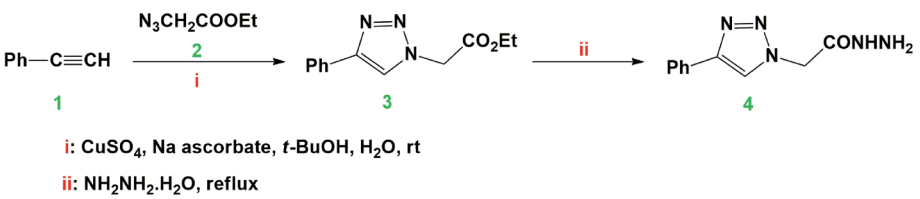

Scheme 1 Synthesis of the 1,2,3-triazole based-ester and/or hydrazide (**3**)/(**4**).

resonated in their appropriate regions.[25] The structures and the IUPAC names of the studied compounds are given in Table 2.

The measurement of the melting points was performed with a Stuart Scientific SMP1. The functional groups were identified using a SHIMADZU FTIR-Affinity-1S spectrometer in the range of 400–4000 cm^{-1}. The measurement of the ^{1}H-NMR (400 MHz) and ^{13}C-NMR (100 MHz) spectra was performed with a Bruker spectrometer (400 MHz). Elemental analyses were performed using a GmbH-Vario EL III Elementar Analyzer.

Synthesis and characterization of ethyl 2-(4-phenyl-1*H*-1,2,3-triazol-1-yl)acetate (3). A mixture of phenylacetylene (**1**) (10 mmol), $CuSO_4 \cdot 5H_2O$ (0.20 g), sodium ascorbate (0.30 g), and ethylazidoacetate (**1**) (12 mmol) in *t*-BuOH : H_2O (1 : 1, v/v) (20 mL) was stirred at room temperature for 4 h. After completion of the reaction, ice cold water (100 mL) was added to the reaction mixture. The formed precipitate was collected by filtration, washed with a saturated solution of ammonium chloride, and recrystallized from ethanol to give the targeted 1,2,3-triazole (**3**).

Yield: 96%, mp: 101–102 °C, IR (ν, cm^{-1}): 1550 (C=C), 1740 (C=O), 2985 (C–H_{al}), 3060 cm^{-1}(C–H_{ar}). ^{1}H-NMR (400 MHz, DMSO-d_6): δ_H = 1.24 (3H, t, J = 4.0 Hz, C**H**$_3$), 4.18–4.22 (2H, q, OC**H**$_2$), 5.14 (s, 2H, NC**H**$_2$), 7.32–7.40 (m, 3H, Ar–H), 7.82–7.90 (m, 2H, Ar–H), 8.50 (s, 1H, CH-1,2,3-triazole). ^{13}C-NMR (100 MHz, DMSO-d_6): δ_C = 14.78 (**C**H$_3$); 51.31 (**N**CH$_2$); 63.40 (**O**CH$_2$); 122.57, 125.70, 127.89, 128.31, 130.98, 146.45 (Ar–C), 166.24 (C=O). Calcd for $C_{12}H_{13}N_3O_2$: C, 62.33; H, 5.67; N, 18.17. Found: C, 62.50; H, 5.59; N, 18.06.

Synthesis and characterization of 2-(4-phenyl-1*H*-1,2,3-triazol-1-yl)acetohydrazide (4). Compound (**3**) (10 mmol) was dissolved in ethanol (30 mL) containing hydrazine hydrate (12 mmol). The mixture was heated under reflux for 4 h. After cooling, the crude product was collected by filtration and recrystallized from ethanol to afford the targeted acid hydrazide (**4**).

Yield: 90%, mp: 185–186 °C, IR (ν, cm^{-1}): 1540 (C=C), 1710 (C=O), 2960 (C–H_{al}), 3080 (C–H_{ar}), 3080 cm^{-1}(N–H). ^{1}H-NMR (400 MHz, DMSO-d_6): δ_H = 4.62 (s, 2H, NH_2), 5.08 (s, 2H, NCH_2), 7.33–7.45 (m, 3H, Ar–H), 7.84–7.87 (m, 2H, Ar–H), 8.54 (s, 1H, CH-1,2,3-triazole), 9.58 (s, 1H, NH). ^{13}C-NMR (100 MHz, DMSO-d_6): δ_C = 51.24 (N**C**H$_2$); 123.14, 125.45, 128.12, 129.45, 130.98, 146.97 (Ar–C), 165.15 (C=O). Calcd for $C_{10}H_{11}N_5O$: C, 55.29; H, 5.10; N, 32.24. Found: C, 55.05; H, 5.18; N, 32.13.

2.2. Materials preparation

The steel used in the present paper is a mild steel composed of Fe (99.21), C (0.21), Mn (0.05), Si (0.38), S (0.05), P (0.09), and Al (0.01). Prior to each experiment, the steel samples were polished with emery paper (until 1500 grid size), washed with distilled water, degreased with acetone, and dried. The molar hydrochloric acid solution was prepared by dilution of analytical grade 37% HCl. The concentration of the studied inhibitors ranged from 5.0×10^{-5} M to 1.0×10^{-3} M.

2.3. Electrochemical study

The electrochemical tests were performed using a potentiostat type VersaSTAT 4, controlled with versa studio analyses software. The various electrochemical experiments were conducted using a three-electrode glass cell. Platinum as the counter electrode, Ag/AgCl as a reference electrode, and mild steel samples as the working electrode. The surface area of the steel electrode used for the electrochemical tests was 1.00 cm^2, and the volume of the solutions used in the glass cell was 50 mL. Prior to the experiments, the potential of the working electrode was stabilized for 30 min until it achieved a stable open circuit potential. The polarization curves were carried out with a scan rate of 1 mV s^{-1} with a potential range of ±250 mV according to the open circuit potential (OCP). The inhibition efficiency (η_{pp}%) was calculated from the corrosion current density values using eqn (1).[26]

$$\eta_{pp}\% = \left[\frac{\left(i^{\circ}_{corr} - i_{corr}\right)}{i^{\circ}_{corr}}\right] \times 100 \quad (1)$$

where i°_{corr} and i_{corr} are the values of the corrosion current densities in the absence and presence of inhibitors, respectively.

On the other hand, the EIS technique were performed in the frequency range from 100 kHz to 100 mHz with 10 points per decade. In this case, the Nyquist plots were plotted and analyzed using a suitable equivalent circuit. The inhibition efficiency was calculated using eqn (2).[27]

$$\eta_{imp}\% = \left[\frac{R'_p - R_p}{R_p}\right] \times 100 \quad (2)$$

where R'_p and R_p are the polarization resistance of the mild steel electrode in the presence and absence of inhibitors, respectively.

2.4. Theoretical approach

Several reactivity descriptors were extracted, such as the highest occupied molecular orbital (HOMO), lowest unoccupied molecular orbital (LUMO), dipole moment (μ), and energy gap (ΔE_{gap}), *etc.* In addition, the reactive sites from electrophilic or nucleophilic attacks were extracted using Fukui indices calculations. These calculations were performed using the Gaussian 09 program[28] at the DFT/(B3LYP) level with the 6-311G (d,p) basis set.

$$\Delta E_{gap} = E_{LUMO} - E_{HOMO} \quad (3)$$

$$\chi = \frac{1}{2}(E_{HOMO} + E_{LUMO}) \quad (4)$$

$$\eta = \frac{1}{2}(E_{HOMO} - E_{LUMO}) \quad (5)$$

$$\sigma = \frac{1}{\eta} \quad (6)$$

The fraction of electrons transferred (ΔN_{110}) from the inhibitor to the (110) surface of the metal was evaluated as reported by Pearson theory:[29]

$$\Delta N_{110} = \frac{\chi_{Fe(110)} - \chi_{inh}}{2(\eta_{Fe(110)} + \eta_{inh})} = \frac{\Phi - \chi_{inh}}{2\eta_{inh}} \quad (7)$$

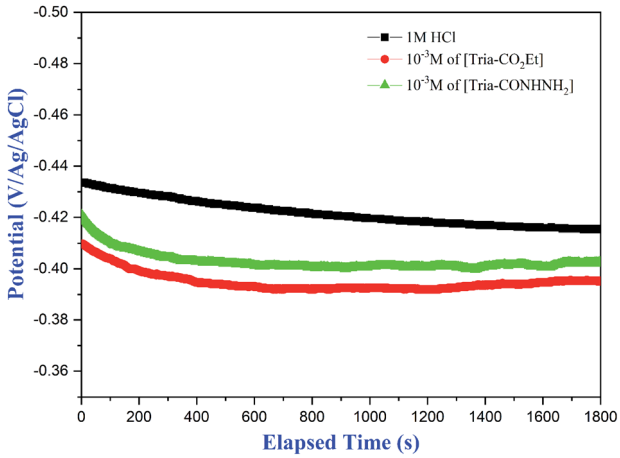

Fig. 1 Evolution of the open circuit potential (OCP) *versus* time for mild steel in 1.0 M HCl at the highest-tested concentration of [Tria-CO_2Et] and [Tria-$CONHNH_2$] at 298 K.

where the work function (Φ) is the theoretical value of the electronegativity on the (110) surface and it presents a dense surface package ($\Phi = \chi_{Fe(110)} = 4.82$ eV). The global hardness corresponding to the metallic bulk is $\eta_{Fe(110)} = 0$ eV.

The Fukui indices indicate a tendency of the molecule to give or obtain electrons. Therefore, these functions have been modeled to detect the most nucleophilic interactions in a molecule.[30] Generally, electrophilic (f_k^-) and nucleophilic (f_k^+) attacks are calculated using eqn (8) and (9):

Nucleophilic attack

$$f_k^+ = P_k(N + 1) - P_k(N) \quad (8)$$

Electrophilic attack

$$f_k^- = P_k(N) - P_k(N - 1) \quad (9)$$

where P_k is the natural population for the atom k site in the cationic ($N - 1$), anionic ($N + 1$), or neutral molecule (N).

3. Results and discussion

3.1. Concentration effect of the studied triazole derivatives

3.1.1. Open circuit potential. The variation of the mild steel potential *versus* the elapsed time during 30 min for the uninhibited solution and the highest-tested concentration of the [Tria-CO_2Et] and [Tria-$CONHNH_2$] inhibitors is illustrated in Fig. 1.

It was noticed that the addition of the studied molecules induces a shift in OCP (*i.e.*, the corrosion potential E_{corr}). Based on the plots presented in Fig. 2, it can be observed that the mild steel sample could achieve a quasi-stable open circuit potential in under 30 min. Therefore, 30 min of OCP measurement was

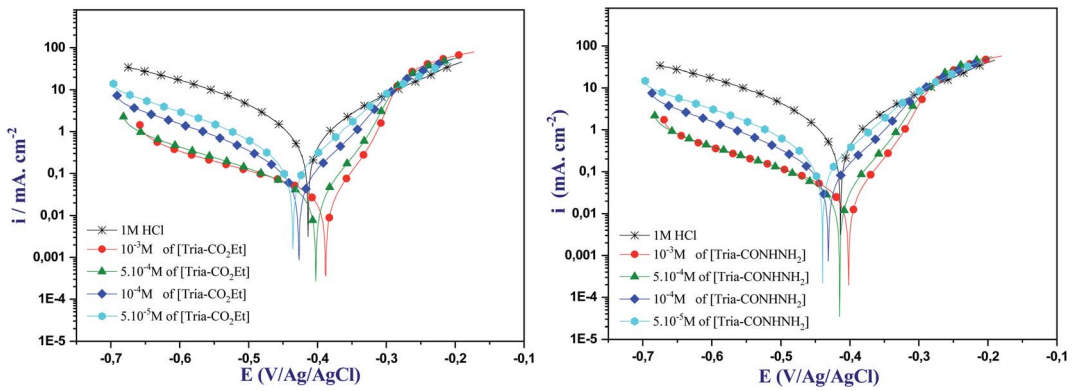

Fig. 2 Polarization curves of mild steel immersed in 1.0 M HCl without and with various concentrations of [Tria-CO_2Et] and [Tria-$CONHNH_2$] at 298 K.

Table 3 Polarization parameters for mild steel in 1.0 M HCl without and with various concentrations of [Tria-CO_2Et] and [Tria-$CONHNH_2$]

Medium	Conc. (M)	$-E_{corr}$ (mV *vs.* Ag/AgCl)	i_{corr} (μA cm^{-2})	$-\beta_c$ (mV dec^{-1})	η_{PP}%
1.0 M HCl	—	413	944	139	—
[Tria-CO_2Et]	5.0×10^{-5}	435	230	138	**75.6**
	1.0×10^{-4}	427	109	138	**88.4**
	5.0×10^{-4}	402	29	136	**96.9**
	1.0×10^{-3}	388	25	130	**97.3**
[Tria-$CONHNH_2$]	5.0×10^{-5}	440	261	138	**72.3**
	1.0×10^{-4}	431	111	138	**88.2**
	5.0×10^{-4}	414	29	137	**96.9**
	1.0×10^{-3}	402	27	137	**97.1**

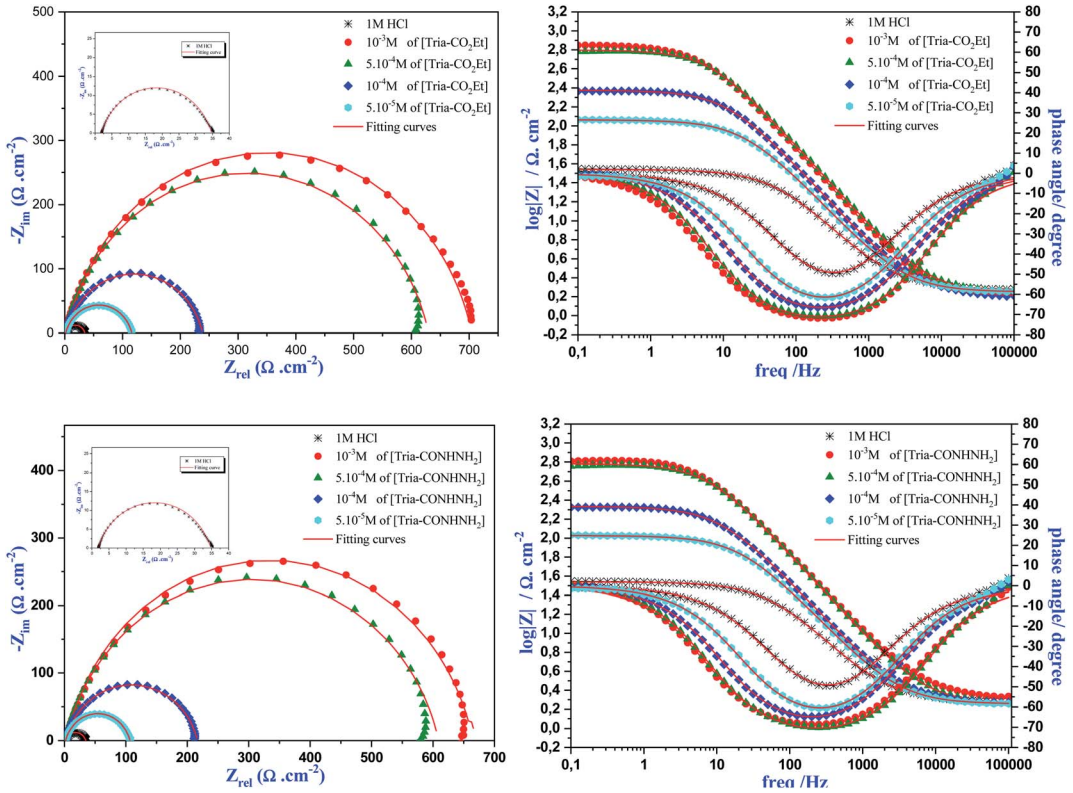

Fig. 3 Nyquist and Bode plots for mild steel in 1.0 M HCl with and without various [Tria-CO_2Et] and [Tria-$CONHNH_2$] concentrations.

Table 4 EIS parameters obtained for mild steel in 1.0 M HCl with and without inhibitors

				CPE				
Medium	Conc (M)	R_s (Ω cm^2)	R_p (Ω cm^2)	Q (μF S^{n-1})	n_{dl}	C_{dl} (μF cm^{-2})	θ	η_{imp} %
1.0 M HCl	—	1.7	33.0	312.7	0.784	89.1	—	—
[Tria-CO_2Et]	5.0×10^{-5}	1.7	114.2	160.7	0.828	70.1	**0.711**	**71.1**
	1.0×10^{-4}	1.6	237.0	116.4	0.838	58.3	**0.860**	**86.0**
	5.0×10^{-4}	1.7	627.8	64.8	0.854	37.5	**0.947**	**94.7**
	1.0×10^{-3}	1.6	702.7	58.9	0.855	34.3	**0.953**	**95.3**
[Tria-$CONHNH_2$]	5.0×10^{-5}	1.7	105.0	165.5	0.824	69.8	**0.685**	**68.5**
	1.0×10^{-4}	1.8	214.9	132.5	0.831	64.3	**0.846**	**84.6**
	5.0×10^{-4}	1.8	607.5	62.3	0.848	34.6	**0.945**	**94.5**
	1.0×10^{-3}	2.1	660.9	57.2	0.866	34.5	**0.950**	**95.0**

assumed prior to performing all electrochemical measurements in this work.

3.1.2. PDP polarization curves. The polarization curves for the mild steel in the presence and absence of [Tria-CO_2Et] and [Tria-$CONHNH_2$] in 1.0 M HCl at 298 K are presented in Fig. 2. Tafel parameters such as the corrosion potential (E_{corr}), corrosion current density (i_{corr}), cathodic Tafel slope (b_c), and percentage inhibition efficiencies (η_{PP}%) are summarized in Table 3.

It can be seen from this figure that the cathodic Tafel slope in the presence of inhibitors decreased obviously to lower values compared to the blank cathodic branches. Also, all curves rise to parallel lines, indicating that our inhibitors do not alter the hydrogen evolution mechanism.[31] In other words, the studied molecules can reduce the hydrogen ions by covering the active reaction sites at the steel surface forming, therefore, a protective film. Moreover, the cathodic slope (b_c) values did not show a large change with the increase of the inhibitor concentration, which indicates that the reduction of hydrogen reaction is investigated according to the pure activation mechanism.[32]

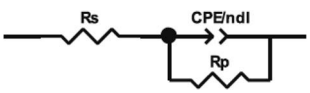

Fig. 4 Electrochemical equivalent circuit used to fit the EIS data.

Table 5 Percentage inhibition efficiency for different heterocyclic compounds in 1.0 M HCl (the concentration used is 1.0×10^{-3} M)

Heterocyclic compound	Highest inhibition efficiency[a] (%)	Metal exposed	Reference
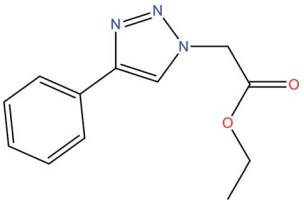 Ethyl 2-(4-phenyl-1*H*-1,2,3-triazol-1-yl)acetate (Tria-CO_2Et)	95.3	Mild steel	This work
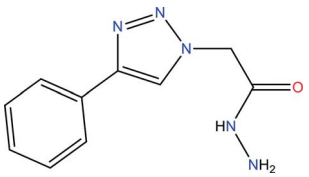 2-(4-Phenyl-1*H*-1,2,3-triazol-1-yl)acetohydrazide (Tria-$CONHNH_2$)	95.0	Mild steel	This work
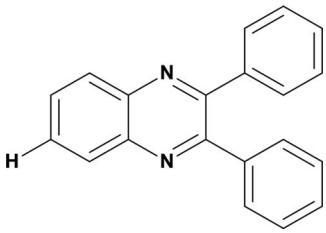 2,3-Diphenylquinoxaline (Q-H)	92.4	Mild steel	39
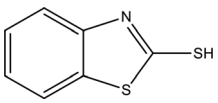 Benzo[*d*]thiazole-2-thiol	86.3	Mild steel	40
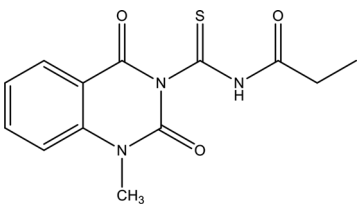 *N*-(1-Methyl-2,4-dioxo-1,2,3,4-tetrahydroquinazoline-3-carbonothioyl)propionamide	88.0	Mild steel	41
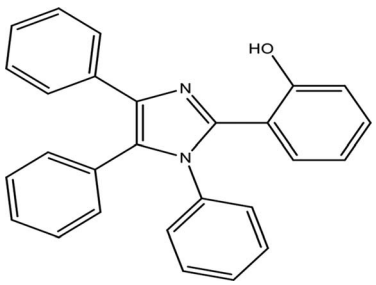 2-(1,4,5-Triphenyl-1*H*-imidazol-2-yl)phenol (P1)	94.0	Mild steel	42
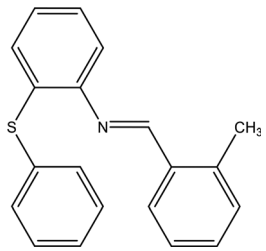 2-(Phenylthio)phenyl-1-(*o*-tolyl)methanimine (PTM)	84.2	Mild steel	43

[a] The inhibition efficiency values were determined using EIS measurements after $\frac{1}{2}$ h of immersion.

Usually, when the E_{corr} displacement is larger than 85 mV, corresponding to that of the uninhibited solution, the inhibitor is regarded as a cathodic- or anodic-type inhibitor. On the other hand, when the displacement is less than 85 mV, the inhibitor is classified as a mixed-type one.[33] In the present paper, the maximum E_{corr} displacements were 25 mV with [Tria-CO_2Et] and 27 mV with [Tria-$CONHNH_2$], suggesting that both inhibitors acted as mixed-type.

3.1.3. EIS measurements. To gain more information about the corrosion mechanisms and confirm the previous results obtained from polarization measurements, EIS measurements were performed. Thus, the Nyquist plots and Bode diagrams (experimental and fit) of the samples in 1.0 M HCl in the presence and absence of the [Tria-CO_2Et] and [Tria-$CONHNH_2$] inhibitors are shown in Fig. 3. In addition, the electrochemical parameters obtained from this technique, and grouped in Table 4, were extracted after a good simulation in the EC-Lab V10.02 software using the electrical equivalent circuit presented in Fig. 4. It can be observed that the presented circuit has a CPE instead of a pure capacitance element since the obtained plots showed a depressed semicircle, non-ideal with their center located below the real axis, which is related to different physical phenomena such as surface heterogeneity.[34]

Moreover, it is clear from Fig. 3 that all of the Nyquist fitted diagrams show a single capacitive loop and the size of these plots increased with the rise of inhibitor concentration, indicating that the corrosion reaction is principally controlled by a charge transfer process.[35] Therefore, this phenomenon is generally shown when we have the dispersal frequency attributed to the surface heterogeneity and roughness of the steel surface.

On the other side, the EIS measurements are presented also in Bode diagrams. The Bode phase angle plots show a single peak at intermediate frequencies, indicating the presence of one time constant. Moreover, the Bode plots obtained in the presence of our inhibitors displayed only one phase maximum, indicating only one relaxation process. Thus, the charge transfer process could have taken place at the metal/electrolyte interface.[36] It is also observed from the Bode plots that a linear relationship between $\log|Z|$ *vs.* $\log(f)$ was shown in the intermittent frequency region, indicating that the phase angle is less than $-90°$ and the slope value is close to -1. These results justified the equivalent circuit obtained.[37]

From Table 4, it can be observed that the R_p values increased with an increase in the [Tria-CO_2Et] and [Tria-$CONHNH_2$] concentration, as well as the inhibition efficiency, which achieved a maximum value of 95.3% for [Tria-CO_2Et] and 95.0% for [Tria-$CONHNH_2$] at the highest-tested concentration (1.0×10^{-3} M). On the other hand, the values of Q and C_{dl} decreased as the concentration of both compounds increased, indicating adsorption on the mild steel surface. Moreover, the n_{dl} values obtained are less than unity in both the inhibited and uninhibited solutions, which indicates that the CPE element acts as a pseudo capacitor.[38] From these results, it can be seen that both studied inhibitors showed a close efficiency despite the replacement of the CO_2Et group by $CONHNH_2$.

Table 5 reports the percentage inhibition efficiency for some selected heterocyclic compounds used as corrosion inhibitors in 1.0 M HCl compared with our compounds (Tria-CO_2Et and Tria-$CONHNH_2$). The values of inhibition efficiency, given in Table 5, were obtained using EIS measurement after 1/2 h of immersion in 1.0 M HCl solution containing 1.0×10^{-3} M of other derivatives. By comparing these data, we can show that our triazole derivatives, Tria-CO_2Et and Tria-$CONHNH_2$, are the most effective inhibitors in 1.0 M HCl. Moreover, triazole derivatives Tria-CO_2Et and Tria-$CONHNH_2$ remain effective against the corrosion of steel at high temperatures (90% at 328 K).

3.1.4. Isotherm adsorption. In order to comprehend the adsorption mechanism of [Tria-CO_2Et] and [Tria-$CONHNH_2$] onto the mild steel surface in the inhibited medium, various isotherm models were tested (Langmuir, Temkin, and Freundlich) using the electrochemical spectroscopy impedance data (Fig. 5). The linear equations of various isotherms are as follows:

Langmuir isotherm:

$$\frac{C_{inh}}{\theta} = \frac{1}{K} + C_{inh};\ \frac{C_{inh}}{\theta}\ \ vs.\ \ C_{inh} \tag{10}$$

Freundlich isotherm:

$$\ln\theta = \ln K + \frac{1}{n}\ln C_{inh};\ \ln(\theta) vs.\ \ln(C_{inh}) \tag{11}$$

Temkin isotherm:

$$\theta = \frac{-1}{2a}\ln(K) - \frac{1}{2a}\ln(C_{inh});\ \theta\ \ vs.\ \ln(C_{inh}) \tag{12}$$

where: θ = the degree of surface coverage. C_{inh} = the inhibitor concentration. K = the equilibrium constant of the adsorption/desorption process. a = the molecular lateral interactions: ($a > 0$; attraction), ($a < 0$; repulsion).

The expression for the standard Gibb's free energy of adsorption, ΔG°_{ads}, was calculated using eqn (13)[44]

$$\Delta G^{\circ}_{ads} = -RT\ln(55.5K) \tag{13}$$

where 55.5 is the molar concentration of H_2O in solution, R is the universal gas constant (8.314 J mol^{-1} K^{-1}), T is the absolute temperature, and K is the equilibrium constant of adsorption/desorption.

Firstly, it is clear from Table 6 that both [Tria-CO_2Et] and [Tria-$CONHNH_2$] obey the Langmuir adsorption isotherm, since they achieve the best regression coefficient (0.999) and a slope close to 1 (1.032 for [Tria-CO_2Et], and 1.033 for [Tria-$CONHNH_2$]).[45] In addition, the adsorption constant values K_{ads} for the Freundlich isotherm are too small to show any significance. Thus, these inhibitors disobey the Freundlich isotherm model. On the other side, the high value of K_{ads} in the Temkin model led us to propose that our compounds might be exhibiting a repulsive interaction, since they have a negative value of the parameter (a) but the regression coefficient is too small compared to those obtained in the Langmuir isotherm, which allowed us to report that [Tria-CO_2Et] and [Tria-$CONHNH_2$] disobey the Temkin isotherm.[46]

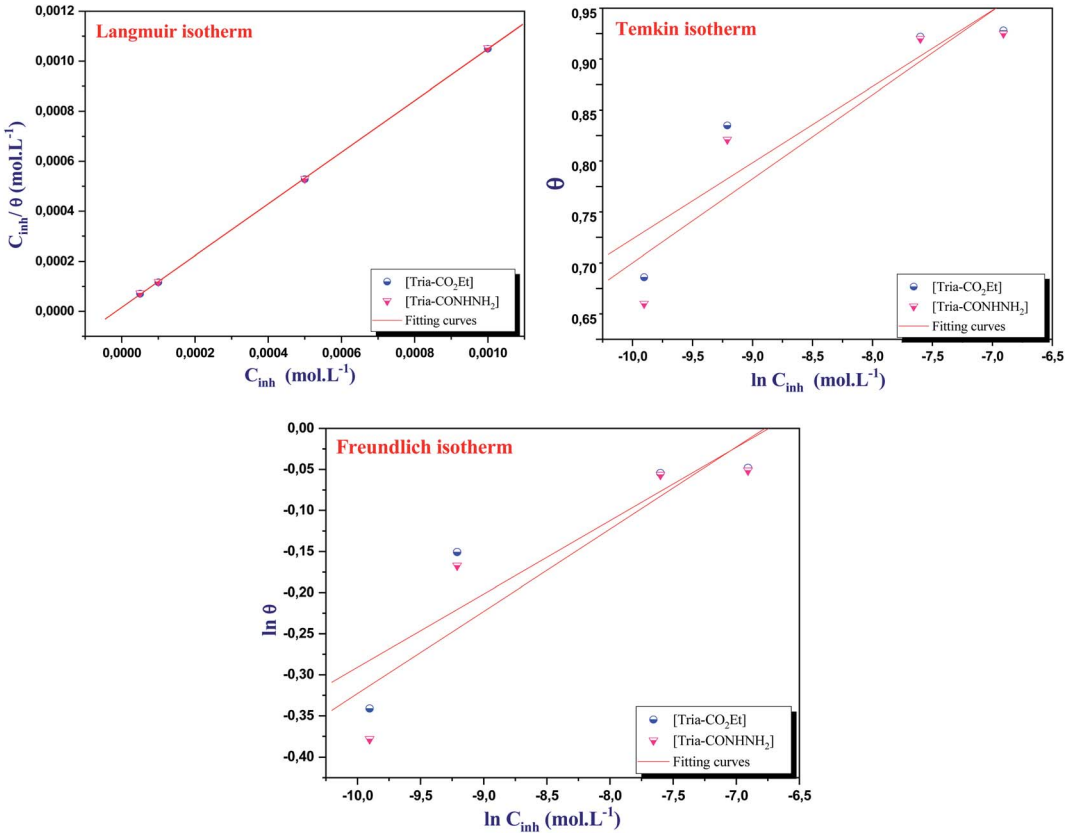

Fig. 5 Langmuir, Freundlich, and Temkin adsorption isotherms of [Tria-CO_2Et] and [Tria-$CONHNH_2$] on the mild steel surface.

Many studies have reported that electrostatic interaction happens between charged molecules and charged metals (physical adsorption) when ΔG_{ads} is around -20 kJ mol^{-1}. Meanwhile, a coordinated bond (chemisorption) is achieved when the ΔG_{ads} values are around -40 kJ mol^{-1} or more.[47,48] In the present work, the ΔG_{ads} values are -37.5 kJ mol^{-1} for [Tria-CO_2Et] and -37.2 kJ mol^{-1} for [Tria-$CONHNH_2$], indicating that our inhibitors adsorbed onto the steel surface by creating a strong barrier film. It has previously been demonstrated that the tested triazole compounds have good corrosion inhibition performances due to their ability to form significant interactions with the iron atoms. It can also be highlighted that in an acidic solution, the surface of the steel electrode takes a positive charge. These actions imply three types of interaction: (i) the interaction of the non-bonding electron pairs on the heteroatoms with the vacant d-orbitals of the Fe-atoms and hence responsible for chemical adsorption. (ii) The interaction occurring between the negatively charged Cl^- ions on the mild steel surface and the positively charged protonated forms of [Tria-$CONHNH_2$] and [Tria-CO_2Et]. (iii) π-electron clouds on the aromatic ring also participating in the donor–acceptor kind of interaction (retro-donation) with the ionized Fe atoms on the surface. These interactions result in the minimization of metal dissolution in the acidic medium by protective film formation of the inhibitor molecules on the mild steel surface.

3.2. Temperature effect of the studied triazole derivatives

Temperature is a valuable parameter in studying the metal corrosion behavior because it can change the electrode/electrolyte interface, such as the dissolution of the adsorbed molecule barrier.[49] Therefore, the effect of temperature on the corrosion inhibition of mild steel in 1.0 M HCl in the absence and presence of 1.0×10^{-3} M [Tria-CO_2Et] and [Tria-$CONHNH_2$] has been investigated at temperatures ranging from 298 K to 328 K using the polarization curve technique. The polarization curves at the highest-tested concentration (1.0×10^{-3} M) are presented in Fig. 6, and the various electrochemical parameters are listed in Table 7.

From the temperature analysis, it can be seen that the i_{corr} values in the presence of the studied inhibitors are less than those obtained in the blank solution, signifying that these compounds have considerably inhibited the corrosion reaction of mild steel. As shown in Table 7, when the temperature is increased from 298 to 328 K, the i_{corr} values are increased from 25 μA cm^{-2} to 270 μA cm^{-2} for [Tria-CO_2Et] and from 27 μA cm^{-2} to 216 μA cm^{-2} for [Tria-$CONHNH_2$]. In addition, it can be noted that the inhibition efficiency decreases slightly in the presence of the inhibitors, so that the two inhibitors remain effective against the corrosion of the steel in hydrochloric acid. Thus, the examined compounds still show superior inhibition performance to protect mild steel from corrosion by forming a firm adsorption film on the steel surface.[49,50]

Table 6 Parameter results from different isotherm models tested

Isotherms	Inhibitors	R^2	Parameters		K	ΔG°_{ads}(kJ mol^{-1})
Langmuir	[Tria-CO_2Et]	0.999	Slope	1.032	6.65×10^4	−37.5
	[Tria-$CONHNH_2$]	0.999		1.033	5.90×10^4	−37.2
Freundlich	[Tria-CO_2Et]	0.907	n	11.19	1.83	−11.4
	[Tria-$CONHNH_2$]	0.908		9.98	1.97	−11.6
Temkin	[Tria-CO_2Et]	0.920	a	−6.68	4.88×10^8	−59.5
	[Tria-$CONHNH_2$]	0.923		−6.06	1.46×10^8	−56.5

The Arrhenius plots of Ln(i_{corr}) *vs.* 1000/T and Ln(i_{corr}/T) *vs.* 1000/T of mild steel in 1.0 M HCl medium containing [Tria-CO_2Et] and [Tria-$CONHNH_2$] are presented in Fig. 7. The corrosion kinetic parameters, such as activation energy (E_a), enthalpy of activation (ΔH_a^*), and entropy of activation (ΔS_a^*) for the corrosion of mild steel in acidic solution without and with the highest-tested concentration of the inhibitors (1.0×10^{-3} M) at temperatures ranging from 298 K to 328 K were calculated from the Arrhenius eqn (14) and the transition state eqn (15).[51] The activation parameters for MS in 1.0 M HCl with and without the studied triazole derivatives are presented in Table 8.

The activation parameters for mild steel in 1.0 M HCl solution without and with the [Tria-CO_2Et] and [Tria-$CONHNH_2$] compounds were obtained from linear square fits of ln I_{corr} *vs.* 1000/T, while the ΔH^* and ΔS^* values were obtained from linear square fits of ln I_{corr}/T *vs.* 1000/T (Fig. 7).

$$i_{corr} = A e^{\left(\frac{-E_a}{RT}\right)} \quad (14)$$

$$i_{corr} = \frac{RT}{N\hbar} e^{\left(\frac{\Delta S^*}{R}\right)} e^{\left(\frac{\Delta H^*}{RT}\right)} \quad (15)$$

where N is Avogadro's number, T is the absolute temperature, R is the gas constant, and $\hbar$ is Plank's constant. From the activation parameter results, it can be seen that the E_a values of the solution containing [Tria-CO_2Et] and [Tria-$CONHNH_2$] are higher than those in the case of the uninhibited solution, which may be attributed to the formation of a compact barrier film on

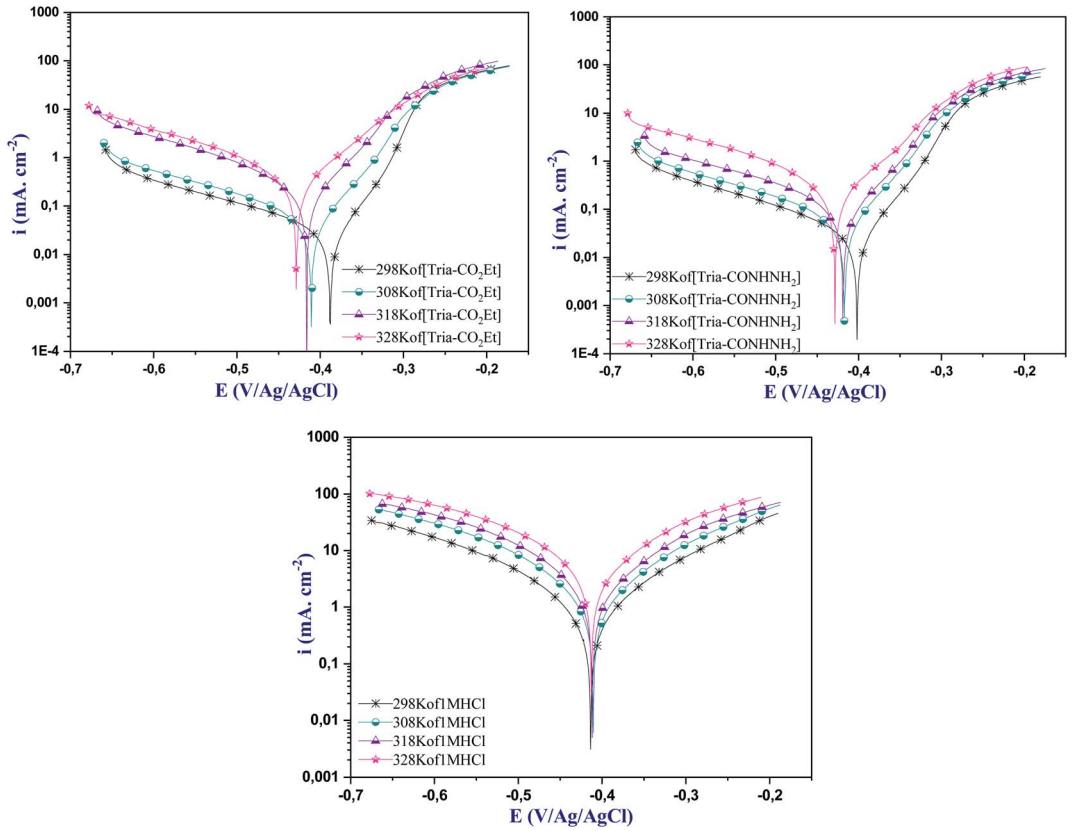

Fig. 6 Polarization curves for steel surfaces without and with the highest-tested concentration of [Tria-CO_2Et] and [Tria-$CONHNH_2$] (1.0×10^{-3} M) at various temperatures.

Table 7 Electrochemical parameters for steel surfaces with and without the studied inhibitors at temperatures ranging from 298 K to 328 K

Medium	Temp. (K)	$-E_{corr}$ (mV *vs.* Ag/AgCl)	i_{corr} (μA cm^{-2})	$-\beta_c$ (mV dec^{-1})	η_{PP}%
1.0 M HCl	298	413	944	139	—
	308	410	1690	137	—
	318	411	2328	126	—
	328	412	3387	120	—
[Tria-CO_2Et]	298	388	25	130	**97.3**
	308	410	46	136	**97.2**
	318	416	170	121	**92.6**
	328	428	270	117	**92.0**
[Tria-$CONHNH_2$]	298	402	27	137	**97.1**
	308	417	49	137	**97.1**
	318	418	86	125	**96.3**
	328	428	216	119	**93.6**

the mild steel surface.[52] The higher energy barrier for the corrosion process in the case of the inhibited solutions suggests that the adsorbed inhibitor film prevents the charge/mass transfer reaction occurring on the surface,[53,54] thus protecting the metal from dissolution. The positive values for the activation enthalpy ΔH_a^* reflect the endothermic nature of the mild steel dissolution process.[55]

The value of activation entropy (ΔS_a^*) increases and is negative in the presence of the inhibitor [Tria-$CONHNH_2$], which means a decrease in the disorder during the transformation of the reagents into an activated complex;[56] in the case of [Tria-CO_2Et] the value of ΔS_a^* was high and positive meaning an increase in the disorder.[53,57]

3.3. DFT study[1]

DFT has been mainly useful to correlate the electronic properties to the inhibition performance obtained experimentally, *i.e.* understanding the adsorption mechanism of the molecules used.[58] Quantum descriptor calculations were extracted using the DFT method at the B3LYP/6-311G (d,p) level (Table 9). The optimized geometries of [Tria-CO_2Et] and [Tria-$CONHNH_2$], as well as their frontier molecular orbitals (LUMO and HOMO), are shown in Fig. 8. The Fukui functions have also been calculated using the natural populations in order to find the most reactive sites of the studied molecules.

From the HOMO and LUMO, the orbital distribution is localized principally in the aromatic and triazole rings showing that [Tria-CO_2Et] and [Tria-$CONHNH_2$] inhibitors can create bonds with the vacant orbital of iron because they have many reactive sites distributed along the inhibitors' structures. Moreover, the ESPM distributions show that the total density (in red color) is located on the oxygen and nitrogen atoms.[59,60] It could be concluded that the present inhibitors can favor the adsorption phenomenon onto the surface of mild steel. The values of the theoretical descriptors obtained for [Tria-CO_2Et] are close to those obtained with [Tria-$CONHNH_2$]. These findings are in good agreement with the experimental results.

Table 8 Thermodynamic parameters of the activation parameters for [Tria-CO_2Et] and [Tria-$CONHNH_2$]

Activation parameters	1.0 M HCl	[Tria-CO_2Et]	[Tria-$CONHNH_2$]
E_a (kJ mol^{-1})	33.8	68.7	55.1
(ΔH_a^*) (kJ mol^{-1})	31.2	66.1	52.5
(ΔH_a^*) (J mol^{-1} K^{-1})	−82.7	3.0	−42.1

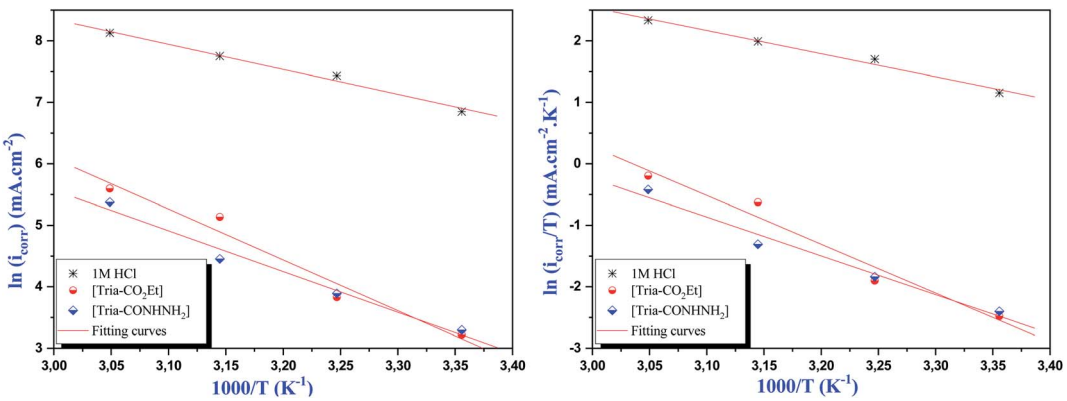

Fig. 7 Arrhenius and transition state plots for mild steel in 1.0 M HCl solution with and without the optimum concentration (1.0×10^{-3} M) of the studied inhibitors.

Table 9 Quantum chemical descriptors for [Tria-CO_2Et] and [Tria-$CONHNH_2$] in the gas and aqueous phases

	[Tria-CO_2Et]		[Tria-$CONHNH_2$]	
Parameters	Gas	Aqueous	Gas	Aqueous
E_{HOMO} (eV)	−6.1183	−6.4269	−6.4427	−6.3763
E_{LUMO} (eV)	−0.7997	−1.0482	−1.0792	−1.0242
ΔE_{gap} (eV)	5.3185	5.3787	5.3634	5.3520
σ (eV^{-1})	0.3760	0.3718	0.3728	0.3736
η (eV)	2.6592	2.6893	2.6817	2.6760
χ (eV)	3.4590	3.7375	3.7609	3.7002
μ (D)	5.2803	7.3222	2.6494	6.3022
ΔN	0.2558	0.2012	0.1974	0.2092
Ω	2.2496	2.5971	2.6372	2.5582
ε	0.4445	0.3850	0.3791	0.3908

According to the obtained E_{HOMO} and ΔE_{gap} values (Table 9), it can be observed that [Tria-CO_2Et] is very reactive in the gas phase, while it is less reactive in the aqueous phase. In addition, it can be suggested that the similar inhibition proprieties of the investigated compounds create this contradiction between the two studied phases. Also, the lower values of E_{LUMO} obtained for both studied molecules indicate the ability of these molecules to accept electrons in the aqueous phase.[61]

Furthermore, the value of $\Delta N_{110} < 3.6$ according to Lukovist's study, signifying the increase in electron-donating ability to the metal surface and this can decrease the corrosion rate of mild steel for both inhibitors.[62] According to the literature, small electronegativity values cause molecules to easily reach electron equilibrium so that the molecules get more reactive. In contrast, high electronegativity values show the opposite. In this study, the electronegativity value of [Tria-CO_2Et] calculated in the gas phase is the lowest (3.45 eV) compared to the electronegativity value for [Tria-$CONHNH_2$], which is 3.76 eV. Based on the dipole moment values in the corrosion field, some authors reported that the dipole moment increases with the efficiency but others say the opposite. In our case, we found that the dipole moment increases with the inhibition efficiency.[63,64]

The most active sites of the Fukui indices for the studied molecules have been extracted in the gas and aqueous phases and are listed in Table 10. It can be seen from these results that the calculated values of f_k^+ for [Tria-CO_2Et] are typically localized on C11, C5, C6, and O16. While, O16, O14, and N4 are the most active sites for electrophilic attack, since the highest values of f_k^- were recorded.[65,66] For [Tria-$CONHNH_2$], the highest values of f_k^+ are situated on the C15, C10, and C5 atoms, which further suggests that these atoms are responsible for forming a back bond by accepting the electron coming from the mild steel surface. However, superior values of f_k^- are on O16, N2, N1, and C15. It can be observed that these responsible sites are also remarked in the aqueous phase and suitable for donor–acceptor

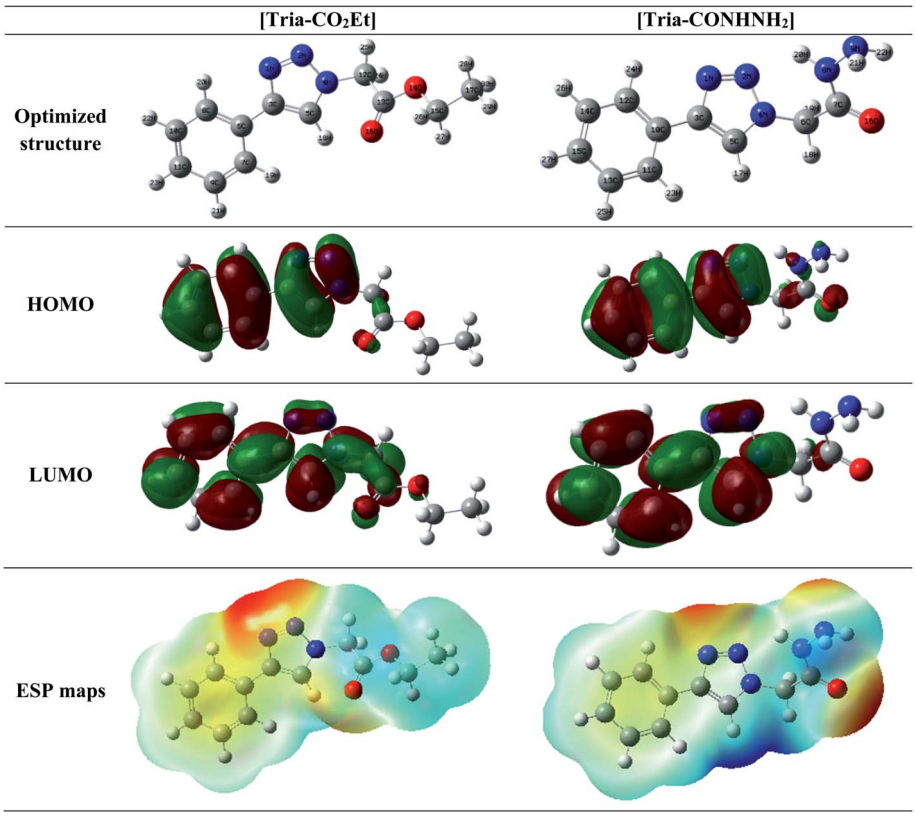

Fig. 8 Optimized structures, HOMO and LUMO and ESP maps for [Tria-CO_2Et] and [Tria-$CONHNH_2$] in neutral form.

Table 10 Most active sites of f_k^+, f_k^- for [Tria-CO_2Et] and [Tria-$CONHNH_2$] in the gas and aqueous phases

Molecule	Atoms	Phase	$P(N)$	$P(N-1)$	$P(N+1)$	f_k^+	f_k^-
[Tria-CO_2Et]	N 1	G	7.265	7.175	7.298	0.033	0.090
		A	7.308	7.221	7.343	0.034	**0.087**
	N4	G	7.157	7.144	7.161	0.003	**1.270**
		A	7.144	7.132	7.155	0.011	0.011
	C5	G	6.097	6.014	6.178	**0.081**	−1.046
		A	6.071	5.968	6.170	**0.099**	**0.103**
	C6	G	6.069	6.023	6.140	**0.070**	0.055
		A	6.077	6.017	6.216	**0.139**	**0.059**
	C 11	G	6.205	6.099	6.318	**0.113**	0.032
		A	6.211	6.103	6.388	**0.177**	**0.108**
	O14	G	8.568	8.520	8.598	0.029	**3.392**
		A	8.562	8.529	8.573	0.011	0.033
	O16	G	8.540	8.446	8.615	**0.075**	**2.500**
		A	8.588	8.499	8.611	0.022	**0.089**
[Tria-$CONHNH_2$]	N 1	G	7.266	7.176	7.296	0.030	0.089
		A	7.311	7.218	7.346	0.034	**0.093**
	N2	G	7.022	6.903	7.051	0.029	**0.118**
		A	7.051	6.915	7.078	0.026	**0.135**
	C 5	G	6.097	6.019	6.186	**0.088**	0.078
		A	6.072	5.983	6.168	**0.095**	**0.088**
	C 10	G	6.069	6.033	6.145	**0.076**	0.035
		A	6.076	6.046	6.235	**0.158**	0.029
	C15	G	6.206	6.108	6.324	**0.118**	**0.097**
		A	6.212	6.136	6.408	**0.196**	0.075
	O 16	G	8.574	8.458	8.6200	0.0458	**0.115**
		A	8.631	8.472	8.6373	0.0059	**0.158**

interactions, and thus facilitate the adsorption of the inhibitor on the metal surface.

4. Conclusion

In the present study, the corrosion inhibition and adsorption characteristics of two triazole derivatives ([Tria-CO_2Et] and [Tria-$CONHNH_2$]) in 1.0 M HCl solution were investigated by various electrochemical techniques and a theoretical approach. The polarization curves display that these compounds acted as a mixed-type inhibitor. The electrochemical impedance spectroscopy results indicate that the inhibition efficiency reaches a maximum value of 95.3% for [Tria-CO_2Et] and 95% for [Tria-$CONHNH_2$]. The temperature study did not show a remarkable effect of the two studied inhibitors in the range of 298–328 K. The adsorption behavior shows that these triazole derivatives suit the Langmuir isotherm model. The obtained global and selective descriptors are in good correlation with the experimental part.

Conflicts of interest

There are no conflicts to declare.

References

1 J. Sharma, S. Ahmad and M. S. Alam, Bioactive triazoles: a potential review, *J. Chem. Pharm. Res.*, 2012, **4**, 5157–5164.
2 N. Phadke Swathi, V. D. P. Alva and S. Samshuddin, A Review on 1,2,4-Triazole Derivatives as Corrosion Inhibitors, *Journal of Bio- and Tribo-Corrosion*, 2017, **3**(4), 42.
3 A. Mohagheghi and R. Arefinia, Corrosion inhibition of carbon steel by dipotassium hydrogen phosphate in alkaline solutions with low chloride contamination, *Constr. Build. Mater.*, 2018, **187**, 760–772.
4 C. Verma, E. E. Ebenso and M. A. Quraishi, Ionic liquids as green and sustainable corrosion inhibitors for metals and alloys: An overview, *J. Mol. Liq.*, 2017, **233**, 403–414.
5 R. Salim, E. Ech-chihbi, H. Oudda, F. El Hajjaji, M. Taleb and S. Jodeh, A review on the assessment of imidazole [1,2-a] pyridines as corrosion inhibitor of metals, *J Bio Tribo. Corros.*, 2019, **13**, 5–11.
6 M. A. Quraishi, D. S. Chauhan, V. S. Saji, *Heterocyclic Corrosion Inhibitors: Principles and Applications*, Elsevier Inc. Amsterdam, 2020.
7 F. El-Hajjaji, M. Messali, M. V. Martínez de Yuso, E. Rodríguez-Castellón, S. Almutairi, T. J. Bandosz and M. Algarra, Effect of 1-(3-phenoxypropyl) pyridazin-1-ium bromide on steel corrosion inhibition in acidic medium, *J. Colloid Interface Sci.*, 2019, **541**, 418–424.
8 M. Ouakki, M. Galai, M. Rbaa, A. S. Abousalem, B. Lakhrissi, E. H. Rifi and M. Cherkaoui, Quantum chemical and experimental evaluation of the inhibitory action of two imidazole derivatives on mild steel corrosion in sulphuric acid medium, *Heliyon*, 2019, **5**, e02759.
9 Q. Ma, S. Qi, X. He, Y. Tang and G. Lu, 1,2,3-Triazole derivatives as corrosion inhibitors for mild steel in acidic medium: Experimental and computational chemistry studies, *Corros. Sci.*, 2017, **129**, 91–101.
10 C. M. Fernandes, L. X. Alvarez, N. E. dos Santos, A. C. Maldonado Barrios and E. A. Ponzio, Green synthesis

of 1-benzyl-4-phenyl-1H-1,2,3-triazole, its application as corrosion inhibitor for mild steel in acidic medium and new approach of classical electrochemical analyses, *Corros. Sci.*, 2019, **149**, 185–194.

11 A. Zarrouk, B. Hammouti, S. S. Al-Deyab, R. Salghi, H. Zarrok, C. Jama and F. Bentiss, Corrosion inhibition performance of 3,5- diamino-1,2,4-triazole for protection of copper in nitric acid solution, *Int. J. Electrochem. Sci.*, 2012, **7**, 5997–6011.

12 R. Salim, A. Elaatiaoui, N. Benchat, E. Ech-chihbi, Z. Rais, H. Oudda, F. El Hajjaji, Y. ElAoufir and M. Taleb, Corrosion behavior of a smart inhibitor in hydrochloric Acid molar: Experimental and theoretical studies, *J. Mech. Eng. Sci.*, 2017, **8**(10), 3747–3758.

13 B. V. A. Rao, M. N. Reddy and B. Sreedhar, Self-assembled 1-octadecyl-1H-1,2,4-triazole films on copper for corrosion protection, *Prog. Org. Coat.*, 2014, **77**, 202–212.

14 T. K. Chaitra, K. N. S. Mohana and H. C. Tandon, Thermodynamic, electrochemical and quantum chemical evaluation of some triazole Schiff bases as mild steel corrosion inhibitors in acid media, *J. Mol. Liq.*, 2015, **211**, 1026–1038.

15 M. El Belghiti, Y. Karzazi, A. Dafali, B. Hammouti, F. Bentiss, I. B. Obot, I. Bahadur and E. E. Ebenso, Experimental, quantum chemical and Monte Carlo simulation studies of 3,5-disubstituted-4-amino-1,2,4-triazoles as corrosion inhibitors on mild steel in acidic medium, *J. Mol. Liq.*, 2016, **218**, 281–293.

16 A. Boutouil, My R. Laamari, I. Elazhary, L. Bahsis, H. Anane and S. E. Stiriba, Towards a deeper understanding of the inhibition mechanism of a new 1,2,3-triazole derivative for mild steel corrosion in the hydrochloric acid solution using coupled experimental and theoretical methods, *Mater. Chem. Phys.*, 2020, **241**, 122420.

17 M. Naciria, Y. El Aoufir, H. Lgaz, F. Lazrak, A. Ghanimi, A. Guenbour, i. H. Alie, M. El Moudanea and T. Jamal, Ill-Min Chung, Exploring the potential of a new 1,2,4-triazole derivative for corrosion protection of carbon steel in HCl: A computational and experimental evaluation, *Colloids Surf., A*, 2020, **597**, 124604.

18 M. Murmu, S. Kr. Saha, P. Bhaumick, N. C. Murmu, H. Hirani and P. Banerjee, Corrosion inhibition property of azomethine functionalized triazole, derivatives in 1 mol L^{-1} HCl medium for mild steel: Experimental and theoretical exploration, *J. Mol. Liq.*, 2020, **313**, 113508.

19 M. R. Aouad, M. Messali, N. Rezki, N. Al-Zaqri and I. Warad, Single proton intramigration in novel 4-phenyl-3-((4-phenyl-1H-1, 2, 3-triazol-1-yl) methyl)-1H-1, 2, 4-triazole-5 (4H)-thione: XRD-crystal interactions, physicochemical, thermal, Hirshfeld surface, DFT realization of thiol/thione tautomerism, *J. Mol. Liq.*, 2018, **264**, 621–630.

20 Y. El Aoufir, R. Aslam, F. Lazrak, R. Marzouki, S. Kaya, S. Skal, A. Ghanimi, I. H. Ali, A. Guenbour, H. Lgaz and I.-M. Chung, The effect of the alkyl chain length on corrosion inhibition performances of 1,2,4-triazole-based compounds for mild steel in 1.0 M HCl: Insights from experimental and theoretical studies, *J. Mol. Liq.*, 2020, **303**, 112631.

21 L. H. Madkour, S. Kaya and I. B. Obot, Computational, Monte Carlo simulation and experimental studies of some arylazotriazoles (AATR) and their copper complexes in corrosion inhibition process, *J. Mol. Liq.*, 2018, **260**, 351–374.

22 Z. Rouifi, F. Benhiba, M. El Faydy, T. Laabaissi, H. About, H. Oudda, I. Warad, A. Guenbour, B. Lakhrissi and A. Zarrouk, Performance and computational studies of new soluble triazole as corrosion inhibitor for carbon steel in HCl, *Chem. Data Collect.*, 2019, **22**, 100242.

23 M. Tourabi, A. Sahibed-dine, A. Zarrouk, I. B. Obot, B. Hammouti, F. Bentiss and A. Nahlé, 3,5-Diaryl-4-amino-1,2,4-triazole Derivatives as Effective Corrosion Inhibitors for Mild Steel in Hydrochloric Acid Solution: Correlation between Anti-corrosion Activity and Chemical Structure, *Prot. Met. Phys. Chem. Surf.*, 2017, **53**(3), 548–559.

24 H. H. Hassan, E. Abdelghani and M. A. Amin, Inhibition of mild steel corrosion in hydrochloric acid solution by triazole derivatives Part I. Polarization and EIS studies, *Electrochim. Acta*, 2007, **52**, 6359–6366.

25 A. Saady, F. El-Hajjaji, M. Taleb, K. IsmailyAlaoui, A. El Biache, A. Mahfoud, G. Alhouari, B. Hammouti, D. S. Chauhan and M. A. Quraishi, Experimental and theoretical tools for corrosion inhibition study of mild steel in aqueous hydrochloric acid solution by new Indanones derivatives, *Mater. Discovery*, 2019, **12**, 30–42.

26 F. El Hajjaji, R. Salim, M. Messali, B. Hammouti, D. S. Chauhan, S. M. Almutairi and M. A. Quraishi, Electrochemical studies on new Pyridazinium derivatives as corrosion inhibitors of carbon steel in acidic medium, *Journal of Bio-and Tribo-Corrosion*, 2019, **5**(1), 4.

27 N. Arrousse, R. Salim, G. A. Houari, F. E. Hajjaji, A. Zarrouk, Z. Rais, D. S. Chauhan and M. A. Quraishi, Experimental and theoretical insights on the adsorption and inhibition mechanism of (2E)-2-(acetylamino)-3-(4-nitrophenyl) prop-2-enoic acid and 4-nitrobenzaldehyde on mild steel corrosion, *J. Chem. Sci.*, 2020, **132**(1), 112.

28 M. Frisch, G. Trucks, H. B. Schlegel, G. Scuseria, M. Robb, J. Cheeseman, G. Scalmani, V. Barone, B. Mennucci, G. Petersson2009, *Gaussian 09, revision a. 02*, Gaussian, Inc., Wallingford, CT, p. 200.

29 A. Singh, K. R. Ansari, A. Kumar, W. Liu, C. Songsong and Y. Lin, Electrochemical, surface and quantum chemical studies of novel imidazole derivatives as corrosion inhibitors for J55 steel in sweet corrosive environment, *J. Alloys Compd.*, 2017, **712**, 121–133.

30 T. Ghailane, R. A. Balkhmima, R. Ghailane, A. Souizi, R. Touir, M. Ebn Touhami, K. Marakchi and N. Komiha, Experimental and theoretical studies for mild steel corrosion inhibition in 1 M HCl by two new benzothiazine derivatives, *Corros. Sci.*, 2013, **76**, 317–324.

31 M. El Faydy, R. Touir, M. Ebn Touhami, A. Zarrouk, C. Jama, B. Lakhrissi, L. O. Olasunkanmi, E. E. Ebenso and F. Bentiss, Corrosion inhibition performance of newly synthesized 5-alkoxymethyl-8-hydroxyquinoline derivatives for carbon steel in 1 M HCl solution: experimental, DFT and Monte

Carlo simulation studies, *Phys. Chem. Chem. Phys.*, 2018, **20**(30), 20167–20187.

32 P. P. Kumari, P. Shetty and S. A. Rao, Electrochemical measurements for the corrosion inhibition of mild steel in 1 M hydrochloric acid by using an aromatic hydrazide derivative, *Arabian J. Chem.*, 2017, **10**, 653–663.

33 T. Ghailane, R. A. Balkhmima, R. Ghailane, A. Souizi, R. Touir, M. Ebn Touhami, K. Marakchi and N. Komiha, Experimental and theoretical studies for mild steel corrosion inhibition in 1 M HCl by two new benzothiazine derivatives, *Corros. Sci.*, 2013, **76**, 317–324.

34 K. Haruna, T. A. Saleh, I. B. Obot and S. A. Umoren, Cyclodextrin-based functionalized graphene oxide as an effective corrosion inhibitor for carbon steel in acidic environment, *Prog. Org. Coat.*, 2019, **128**, 157–167.

35 A. Zarrouk, B. Hammouti, T. Lakhlifi, M. Traisnel, H. Vezin and F. Bentiss, New 1Hpyrrole- 2, 5-dione derivatives as efficient organic inhibitors of carbon steel corrosion in hydrochloric acid medium: electrochemical, XPS and DFT studies, *Corros. Sci.*, 2015, **90**, 572–584.

36 Y. W. Liu, Y. Chen, X. H. Chen, Z. N. Yang and Z. Zhang, Study on adsorption behavior of ketoconazole on Q235 mild steel in 1.0M HCl solution with electrochemical measurement, *J. Alloys Compd.*, 2018, **758**, 184–193.

37 C. Verma, M. A. Quraishi and A. Singh, 5-substituted 1H-tetrazoles as effective corrosioninhibitors for mild steel in 1M hydrochloric acid, *J. Taibah Univ. Sci.*, 2016, **10**, 718–733.

38 E. Ech-chihbi, A. Nahlé, R. Salim, H. Oudda, F. El Hajjaji, F. El Kalai, A. El Aatiaoui and M. Taleb, An Investigation into Quantum Chemistry and Experimental Evaluation of Imidazopyridine Derivatives as Corrosion Inhibitors for C-Steel in Acidic Media, *Journal of Bio- and Tribo-Corrosion*, 2019, **5**(1), 24.

39 M. Ouakki, M. Galai, Z. Benzekri, C. Verma, E. Ech-chihbi, S. Kaya, S. Boukhris, E. E. Ebenso, M. Ebn Touhami and M. Cherkaoui, Insights into corrosion inhibition mechanism of mild steel in 1 M HCl solution by quinoxaline derivatives: electrochemical, SEM/EDAX, UV-visible, FT-IR and theoretical approaches, *Colloids Surf., A*, 2021, **611**, 125810.

40 F. Benhiba, Z. Benzekri, A. Guenbour, M. Tabyaoui, A. Bellaouchou, S. Boukhris and A. Zarrouk, Combined electronic/atomic level computational, surface (SEM/EDS), chemical and electrochemical studies of the mild steel surface by quinoxalines derivatives anti-corrosion properties in 1 mol L-1 HCl solution, Chin, *J. Chem. Eng.*, 2020, **28**, 1436–1458.

41 Y. El Aoufir, R. Aslam, F. Lazrak, R. Marzouki, S. Kaya, S. Skal and I. M. Chung, The effect of the alkyl chain length on corrosion inhibition performances of 1, 2, 4- triazole-based compounds for mild steel in 1.0 M HCl: Insights from experimental and theoretical studies, *J. Mol. Liq.*, 2020, **303**, 112631.

42 M. Ouakki, M. Galai, M. Rbaa, A. S. Abousalem, B. Lakhrissi, M. Ebn Touhami and M. Cherkaoui, Electrochemical, thermodynamic and theoretical studies of some imidazole derivatives compounds as acid corrosion inhibitors for mild steel, *J. Mol. Liq.*, 2020, **319**, 114063.

43 H. Keles, D. M. Emir and M. Keles, A comparative study of the corrosion inhibition of low carbon steel inHCl solution by an imine compound and its cobalt complex, *Corros. Sci.*, 2015, **101**, 19–31.

44 N. Arrousse, R. Salim, Y. Kaddouri, A. Zarrouk, D. Zahri, F. El Hajjaji, R. Touzani, M. Taleb and S. Jodeh, The inhibition behavior of two pyrimidine-pyrazole derivatives against corrosion in hydrochloric solution: Experimental, surface analysis and in silico approach studies, *Arabian J. Chem.*, 2020, **13**(7), 5949–5965.

45 E. Ituen, O. Akaranta and A. James, Evaluation of Performance of Corrosion Inhibitors Using Adsorption Isotherm Models: An Overview, *Chem. Sci. Int. J.*, 2017, **18**(1), 1–3.

46 C. Verma, L. O. Olasunkanmi, I. Bahadur, H. Lgaz, M. A. Quraishi, J. Haque, M. El-Sayed, M. Scherif and E. E. Ebenso, Experimental, density functional theory and molecular dynamics supported adsorption behavior of environmental benign imidazolium based ionic liquids on mild steel surface in acidic medium, *J. Mol. Liq.*, 2019, **273**, 1–15.

47 F. El-Hajjaji, M. Messali, A. Aljuhani, M. R. Aouad, B. Hammouti, M. E. Belghiti, D. S. Chauhan and M. A. Quraishi, *J. Mol. Liq.*, 2018, **249**, 997–1008.

48 D. A. Teixeira, M. A. G. Valente, Jr. Assis, V. Benedetti, G. T. Feliciano, S. C. da Silvac and C. S. Fugivara, Experimental and Theoretical Studies of Volatile Corrosion Inhibitors Adsorption on Zinc Electrode, *J. Braz. Chem. Soc.*, 2015, **26**(3), 434–450.

49 K. Zhang, B. Xu, W. Yang, X. Yin, Y. Liu and Y. Chen, Halogen-substituted imidazoline derivatives as corrosion inhibitors for mild steel in hydrochloric acid solution, *Corros. Sci.*, 2014, **90**, 284–295.

50 H. Hamani, T. Douadi, D. Daoud, M. Al Noaimi, R. A. Rikkouh and S. Chafaa, 1-(4- Nitrophenyloimino)-1-(phenylhydrazono)-propan-2-one as corrosion inhibitor for mild steel in 1M HCl solution: weight loss, electrochemical, thermodynamic and quantum chemical studies, *J. Electroanal. Chem.*, 2017, **801**, 425–438.

51 A. Dutta, S. K. Saha, P. Banerjee and D. Sukul, Correlating electronic structure with corrosion inhibition potentiality of some bis-benzimidazole derivatives for mild steel in hydrochloric acid: combined experimental and theoretical studies, *Corros. Sci.*, 2015, **98**, 541–550.

52 E. Ech-chihbi, M. E Belghiti, R. Salim, H. Oudda, M. Taleb, N. Benchat, B. Hammouti and F. El-Hajjaji, Experimental and computational studies on the inhibition performance of the organic compound "2-phenylimidazo [1,2-a] pyrimidine-3- carbaldehyde" against the corrosion of carbon steel in 1.0 M HCl solution, *Surf. Interfaces*, 2017, **9**, 206–217.

53 M. Ouakki, M. Galai, M. Rbaa, A. S. Abousalem, B. Lakhrissi, E. H. Rifi and M. Cherkaoui, Investigation of imidazole derivatives as corrosion inhibitors for mild steel in sulfuric

acidic environment: experimental and theoretical studies, *Ionics*, 2020, **26**, 5251–5272.

54 L. C. Murulana, M. M. Kabanda and E. E. Ebenso, Investigation of the adsorption characteristics of some selected sulphonamide derivatives as corrosion inhibitors at mild steel/hydrochloric acid interface: Experimental, quantum chemical and QSAR studies, *J. Mol. Liq.*, 2016, **215**, 763–779.

55 M. El Hezzat, M. Assouag, H. Zarrok, Z. Benzekri, A. El Assyry, S. Boukhris, A. Souizi, M. Galai, R. Touir, M. Ebn Touhami, H. Oudda and A. Zarrouk, Correlated DFT and electrochemical study on inhibition behavior of ethyl 6-amino-5-cyano-2-methyl-4-(p-tolyl)-4H-pyran-3-carboxylate for the corrosion of mild steel in HCl, *Der Pharma Chem.*, 2015, **7**(10), 77–88.

56 M. Yadav, S. Kumar, N. Tiwari, I. Bahadur and E. E. Ebenso, Experimental and quantum chemical studies of synthesized triazine derivatives as an efficient corrosion inhibitor for N80 steel in acidic medium, *J. Mol. Liq.*, 2015, **212**, 151–167.

57 M. Elachouri, M. S. Hajji, M. Salem, S. Kertit, J. Aride, R. Coudert and E. Essassi, Some Nonionic Surfactants as Inhibitors of the Corrosion of Iron in Acid Chloride Solutions, *Corrosion*, 1996, **52**(2), 103–108.

58 A. S. El-Tabei, E. A. Elsharaky and A. E. El-Tabey, A comparative the inhibition performance of a newly synthesized cationic surfmer and its oligomer surfactant for carbon steel corrosion in 1M acid chloride solution, *Int. J. Electrochem. Sci.*, 2016, **11**(12), 10978–11001.

59 A. Bendjeddou, T. Abbaz, A. Gouasmia and K. D. Villemin, Molecular structure, HOMO LUMO, MEP and Fukui function analysis of some TTF-donor substituted molecules using DFT (B3LYP) calculations, *Int. Res. J. Pure Appl. Chem.*, 2016, **12**(1), 1–9.

60 A. Zarrouk, H. Zarrok, Y. Ramli, M. Bouachrine, B. Hammouti, A. Sahibed-dine and F. Bentiss, Inhibitive properties, adsorption and theoretical study of 3,7-dimethyl-1-(prop-2-yn-1-yl)quinoxalin-2(1H)-one as efficient corrosion inhibitor for carbon steel in hydrochloric acid solution, *J. Mol. Liq.*, 2016, **222**, 239–252.

61 G. Raja, K. Saravanan and S. Sivakumar, Quantum chemical investigations on benzene derivative: a DFT study, *Rasayan J. Chem.*, 2015, **8**(1), 37–41.

62 K. Sayin and D. Karakas, Ab-initio and DFT calculations on some inorganic inhibitors computational study on inorganic corrosion inhibitors, *J New Results Sci*, 2017, **6**(1), 20–31.

63 M. Yadav, S. Kumar, R. R. Sinha and D. Behera, Experimental and quantum chemical studies on the corrosion inhibition performance of benzimidazole derivatives for mild steel in HCl, *Ind. Eng. Chem. Res.*, 2013, **52**(19), 6318–6328.

64 F. El Hajjaji, E. Ech-chihbi, N. Rezki, F. Benhiba, M. Taleb, D. S. Chauhan and M. A. Quraishi, Electrochemical and theoretical insights on the adsorption and corrosion inhibition of novel pyridinium-derived ionic liquids for mild steel in 1 M HCl, *J. Mol. Liq.*, 2020, **314**, 113737.

65 L. Guo, S. Kaya, I. B. Obot, X. Zheng and Y. Qiang, Toward understanding the anticorrosive mechanism of some thiourea derivatives for carbon steel corrosion: A combined DFT and molecular dynamics investigation, *J. Colloid Interface Sci.*, 2017, **506**, 478–485.

66 E. Ech-chihbi, A. Nahlé, R. Salim, F. Benhiba, A. Moussaif, F. El-Hajjaji, H. Oudda, A. Guenbour, M. Taleb, I. Warad and A. Zarrouk, Computational, MD simulation, SEM/EDX and experimental studies for understanding adsorption of benzimidazole derivatives as corrosion inhibitors in 1.0 M HCl solution, *J. Alloys Compd.*, 2020, **20**, 155842.